Journal of Geoscience and Environment Protection, 2025, 13(4), 49-79
https://www.scirp.org/journal/gep
ISSN Online: 2327-4344
ISSN Print: 2327-4336

Spatial and Temporal Trends of Extreme Precipitation in Eastern Africa during January 1981-2023

Daniel Jonathan Masunga[1,2,3], Ling Zhang[1], Conteh Moneh[2], Nestory Silvestry Mosha[2,3], Daniel Gibson Mwageni[2,3], Innocent Junior[2]

[1]Key Laboratory of Meteorology Disaster, Ministry of Education (KLME)/Joint International Research Laboratory of Climate and Environment Change (ILCEC)/Collaborative Innovation Center on Forecast and Evaluation of Meteorological Disasters (CIC-FEMD), Nanjing University of Information Science and Technology, Nanjing, China
[2]School of Atmospheric Sciences, Nanjing University of Information Science and Technology, Nanjing, China
[3]Tanzania Meteorological Authority (TMA), Dodoma, Tanzania
Email: danielmasunga55@gmail.com, daniel.masunga@meteo.go.tz

How to cite this paper: Masunga, D. J., Zhang, L., Moneh, C., Mosha, N. S., Mwageni, D. G., & Junior, I. (2025). Spatial and Temporal Trends of Extreme Precipitation in Eastern Africa during January 1981-2023. *Journal of Geoscience and Environment Protection, 13,* 49-79.
https://doi.org/10.4236/gep.2025.134004

Received: March 10, 2025
Accepted: April 7, 2025
Published: April 10, 2025

Abstract

Extreme precipitation events pose significant challenges to water resources, agriculture, infrastructure, public health, ecosystems, energy production, fishing, timber production, and other rain-dependent socioeconomic sectors across Eastern Africa, threatening the environment and regional livelihoods. This study analyzes spatial and temporal trends of extreme precipitation in Eastern Africa from January 1981 to 2023, using high-resolution CHIRPS data. Key extreme precipitation indices, including R10mm, R75p, and SDII, were calculated to assess variations in the frequency, intensity, and contribution of extreme rainfall events. The temporal analysis reveals a statistically significant increasing trend in January precipitation (0.844 mm/year, $p = 0.0191$), confirmed by Sen's Slope (0.74 mm/year). R10mm increased by 0.036 days/year ($p = 0.0079$), with Sen's Slope estimating 0.04 days/year. R75p showed a rise of 0.025 days/year ($p = 0.0113$), with Sen's Slope at 0.02 days/year. SDII exhibited the most significant trend, increasing by 0.056 mm/day per year ($p = 0.0002$), with Sen's Slope at 0.06 mm/day per year. These results indicate a rise in extreme precipitation in Eastern Africa, increasing the risk of flooding and other climate-related hazards. Spatial analysis shows distinct regional variations, with Southern Tanzania, Mozambique, Malawi, Zambia, Zimbabwe, and Madagascar exhibiting statistically significant increasing trends in January precipitation and extreme precipitation indices. These regions are becoming more vulnerable to flooding and other climate-related hazards. Moreover, correlation analysis identifies significant links between global SST anomalies and extreme precipitation trends, demonstrating the influence of large-scale climate drivers.

The study indicates the growing intensity and frequency of extreme precipitation in parts of Eastern Africa, significantly influenced by the South Pacific Convergence Zone (SPCZ). This necessitates a deeper understanding of SPCZ dynamics and their impacts on precipitation patterns to enhance climate prediction and develop adaptive strategies for mitigating extreme weather events. Such efforts will contribute to safeguarding water resources, agriculture, infrastructure, public health, energy production, fisheries, transportation, and livelihoods across the region.

Keywords

Extreme Precipitation, Temporal Trend, Spatial Trend, Eastern Africa, SPCZ

1. Introduction

Precipitation is a fundamental component of the hydrological cycle, sustaining ecosystems, agricultural productivity, and livelihoods on a global scale. In Eastern Africa, a region heavily reliant on rainfall for agriculture and water resources, precipitation patterns directly influence food security, energy production, and socio-economic stability. However, the region faces significant climatic variability, with extreme precipitation events, such as heavy rainfall and prolonged droughts, frequently disrupting the region's delicate balance. These changes have far-reaching consequences on both the environment and the economy, affecting various sectors in complex ways (IPCC, 2021; Nicholson, 2017; Funk et al., 2019).

Extreme precipitation events in Eastern Africa have significant environmental, societal, and economic consequences, including floods, landslides, and dry spells (Shongwe et al., 2011; Niang et al., 2014; Otieno & Anyah, 2013). Given the region's dependence on rain-fed agriculture, precipitation patterns jeopardize food production, increase the risk of water scarcity, and exacerbate social inequalities. Analyzing the spatial and temporal trends of extreme precipitation is key to effective and sustainable water resource management, agricultural planning, disaster risk reduction, and the development of effective climate adaptation strategies, particularly in light of the growing impacts of climate change (Conway & Schipper, 2011; IPCC, 2021).

Eastern Africa's substantial climatic variability, high population density, and socio-economic disparities heighten its vulnerability to extreme weather events, including shifts in precipitation patterns (Ayugi et al., 2022; Pereira, 2017). Rapid population growth, particularly in Tanzania, Kenya, Uganda, and Rwanda, increases pressure on land and water resources, leading to environmental degradation. Unsustainable practices such as deforestation and overgrazing further weaken the region's resilience, amplifying the impacts of extreme precipitation events (Msofe et al., 2020).

Extreme precipitation events, including heavy rainfall and prolonged droughts, pose significant threats to the livelihoods and well-being of Eastern African pop-

ulations (Haile et al., 2020). These events can have devastating consequences, severely affecting livelihoods and disrupting multiple sectors. Intense rainfall can overwhelm drainage systems, causing widespread flooding that damages infrastructure, disrupts agricultural activities, and leads to displacement and loss of life. The intensity of these events can be exacerbated by factors like deforestation and soil degradation, further compounding their negative impacts. Conversely, prolonged periods of low rainfall result in severe droughts, leading to crop failures, livestock losses, water scarcity, and an increased risk of famine (Haile et al., 2020; Mokria et al., 2017). Drought can have particularly severe impacts on already vulnerable communities that depend heavily on rain-fed agriculture (Teshome & Zhang, 2019).

The region's agricultural and hydrological systems are highly sensitive to extreme precipitation, with far-reaching effects on food security and water resources (Cai et al., 2015). Prolonged droughts, often exacerbated by the warming climate, reduce agricultural productivity (Müller et al., 2011; Mafie, 2022), endangering the livelihoods of smallholder farmers. These farmers, who form the backbone of the region's economy, are especially vulnerable to unpredictable rainfall (Schlenker & Lobell, 2010; Morton, 2007; Cooper et al., 2008; Rowhani et al., 2011). Conversely, intense rainfall events, while beneficial for replenishing water resources, often result in floods that damage crops, infrastructure, and homes (Di Baldassarre et al., 2010; Field et al., 2014; Chang'a et al., 2020). Floods disrupt transportation, destroy agricultural fields, and exacerbate the spread of waterborne diseases such as diarrhea, cholera, typhoid fever, and malaria.

Climate change is expected to further influence extreme precipitation trends. Studies project increasing temperatures and changing precipitation patterns (Osima et al., 2018). Rising global temperatures intensify the hydrological cycle by increasing atmospheric moisture capacity, leading to heavier and more frequent rainfall events (Allan et al., 2010; Kijazi & Reason, 2009; Trenberth, 2011). Tropical and subtropical regions, including Eastern Africa, are particularly vulnerable to these changes, with a rising frequency of catastrophic floods driven by both warming-induced shifts and natural climate variability (Chang'a et al., 2020; Pascale et al., 2016; Taylor et al., 2017). These trends stress the need for effective climate risk management strategies.

The hydrological and climatic variability of Eastern Africa is shaped by complex interactions among atmospheric circulation patterns, ocean-atmosphere coupling, and regional factors such as topography, forests, and the effects of water bodies. The region's diverse climatic zones are influenced by key atmospheric systems, including the Intertropical Convergence Zone (ITCZ), the Indian Ocean Dipole (IOD), and the El Niño-Southern Oscillation (ENSO). These systems, coupled with local weather dynamics, have a strong impact on rainfall patterns across the region (Kebacho, Ongoma, & Chen, 2024; Ingeri et al., 2024; Pierre Camberlin, 2018; Schott, Xie, & McCreary, 2009). The impact of these climate systems on precipitation varies across the region, with coastal areas often experiencing differ-

ent effects from the interior highlands.

Previous studies have examined various aspects of extreme precipitation in Eastern Africa, but a comprehensive analysis covering the entire region from January 1981 to December 2023 is still lacking. Many studies have focused on specific sub-regions or shorter periods, using different methodologies and datasets. For example, Ayugi et al. (2022) analyzed extreme precipitation indices in East Africa under 1.5˚C and 2.0˚C global warming levels, finding that population exposure to extreme precipitation is more strongly influenced by demographic changes than by climate-related factors alone. However, the geographical scope of this study is narrower than the scope of the current research. Other studies have examined the projected impacts of climate change on drought patterns in East Africa (Haile et al., 2020), focusing on changes in drought area, frequency, duration, and intensity across various sub-regions.

Despite significant research efforts, long-term, region-wide studies on extreme precipitation trends remain limited, hindering the development of effective climate adaptation strategies and evidence-based policymaking. The localized nature of extreme events, such as floods in some areas and droughts in others, calls for a more detailed understanding of precipitation patterns, influenced by factors like topography, proximity to water bodies, and regional climate dynamics.

This study seeks to address these gaps by analyzing the spatial and temporal trends of extreme precipitation across Eastern Africa from January 1981 to December 2023. By utilizing high-resolution precipitation datasets and advanced statistical methods, the research seeks to identify underlying patterns and examine correlations between extreme precipitation events and global sea surface temperature (SST) anomalies. The findings will clarify how specific oceanic regions influence extreme precipitation patterns, enhancing the predictability of such events and strengthening climate risk management. This knowledge will contribute to developing early warning systems and shaping effective climate adaptation and disaster risk reduction strategies. Moreover, the study's results will serve as a valuable resource for policymakers, researchers, and practitioners committed to improving climate resilience in the region.

2. Study Area, Data, and Methodology

2.1. Study Area

Eastern Africa is a geographically and climatically diverse region. For this study, the region comprises several countries, including Tanzania, Kenya, Uganda, Rwanda, Burundi, Malawi, Zambia, Zimbabwe, Mozambique, and Madagascar (**Figure 1**). The region spans latitudes from approximately 4˚40' N to 26˚52' S and longitudes from 22˚00' E to 50˚40' E, encompassing a wide range of ecosystems, including expansive savannas, coastal plains, highland plateaus, and towering mountain ranges. This diversity in topography and geography strongly influences its complex climatic patterns and varied precipitation regimes.

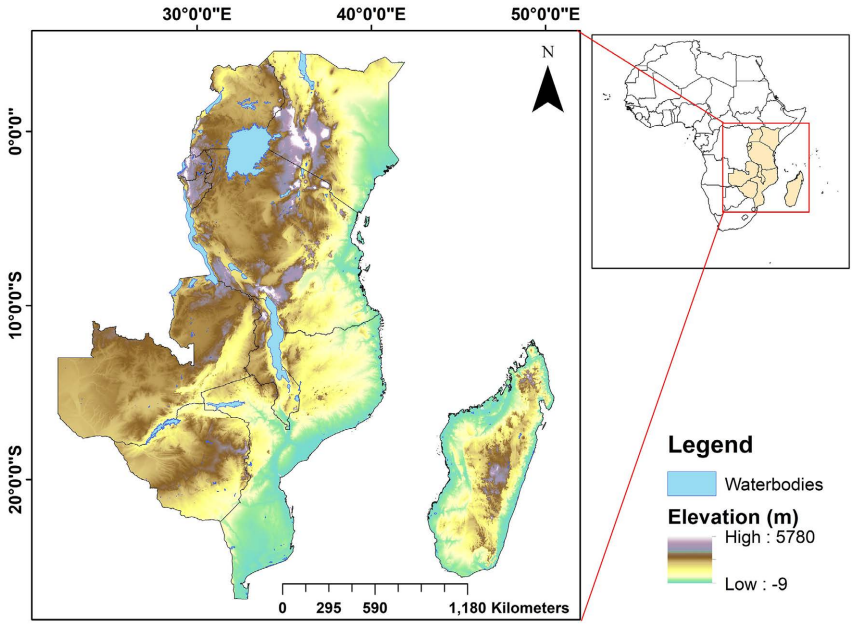

Figure 1. Geographic representation of the study area. (Left) Map of Eastern Africa, depicting altitude variations across the region, with darker shades representing higher elevations. Notable features include Mount Kilimanjaro in Tanzania, the tallest mountain in Africa. (Right) Location of Eastern Africa within the African continent.

Massive forests, particularly the Congo Rainforest, significantly impact precipitation patterns in Eastern Africa by acting as critical moisture sources and influencing regional atmospheric circulation. The Congo Forest generates substantial evapotranspiration, releasing vast amounts of water vapor into the atmosphere, which contributes to cloud formation and rainfall (Washington et al., 2013; Werth & Avissar, 2002) This moisture is transported by prevailing westerly winds, particularly affecting the western and central parts of the region, where it enhances precipitation in areas downwind of the forest. Additionally, these forests influence atmospheric circulation by creating low-pressure systems that attract moist air masses, further amplifying rainfall. However, deforestation can disrupt these moisture cycles, reducing precipitation and exacerbating the frequency and intensity of extreme weather events (Lawrence & Vandecar, 2015). The interplay between the Indian Ocean's climatic drivers and the Congo Forest's moisture contributions creates a complex and dynamic rainfall pattern across Eastern Africa.

Prominent geographic features such as Mount Kilimanjaro in Tanzania, the highest mountain in Africa at 5895 meters, and Mount Kenya in Kenya contribute significantly to local and regional precipitation patterns (Hastenrath, 2001; Kijazi & Reason, 2009). These towering peaks, along with other highlands like the Nyungwe and Virunga ranges in Rwanda, the Kibira Highlands in Burundi and the central highlands of Madagascar (Plumptre et al., 2007; Vande Weghe, 2004) act as orographic barriers. These barriers force moist air from the Indian Ocean to rise, cool, and condense, resulting in increased rainfall on the windward slopes and creating drier conditions on the leeward sides. The Great Rift Valley further

introduces localized rainfall variations in the region, primarily due to orographic lifting and rain-shadow effects, especially in areas with steep escarpments.

In Madagascar, the central highlands not only contribute to orographic precipitation but also influence local climatic conditions, with moist winds from the Indian Ocean depositing rainfall on eastern slopes while leaving western regions relatively arid (Donque, 1972). The combined effects of these geographic features contribute to the region's highly complex precipitation patterns and climatic variability, necessitating detailed analysis to understand extreme precipitation trends.

The region is home to some of the world's most significant inland water bodies. Lake Victoria, the largest tropical lake and the second-largest freshwater lake by surface area globally, substantially influences local convection and rainfall patterns (Anyah & Semazzi, 2004; Song et al., 2004). Lake Tanganyika, Africa's deepest lake and one of the oldest lakes on Earth, alongside Lake Nyasa, known for its extraordinary biodiversity, contributes to the development of localized microclimates (O'Reilly et al., 2003; Verburga & Hecky, 2009). These lakes enhance precipitation dynamics through lake-induced convection, where the differential heating of water and land surfaces intensifies moisture availability and generates localized rainfall in adjacent regions.

Rainfall seasonality varies across the region. In Kenya, Uganda, and Tanzania, two main rainy seasons occur: the long rains (March-May (MAM)) and the short rains (October-December (OND)) (Camberlin & Okoola, 2003; Nicholson, 2017). In Mozambique and southern Madagascar, rainfall peaks during the austral summer (November-April), with the most intense rains from December to February. Northern Madagascar experiences relatively consistent rainfall year-round, with a distinct wet season from November to April (Reason & Keibel, 2004; Jury, 2013). Rwanda experiences a long rainy season (MAM) and a short rainy season (September-December (SOND)). In Burundi, there is a short dry season from December to January, followed by a long rainy season from February to May. Between May and October, precipitation remains low, with June to August often being completely dry, before substantial rains return from October to December (Sebaziga et al., 2024). Zambia and Zimbabwe experience a more defined wet season from November to March. In contrast, Burundi and Rwanda, located in the highland regions, experience relatively evenly distributed rainfall throughout the year, with less pronounced seasonal variations compared to other parts of the region.

Additionally, countries such as Mozambique and Madagascar are heavily influenced by tropical cyclones, which significantly affect their rainfall distribution and flood risks. These nations face the compounded challenge of dealing with cyclones that have increased in frequency and intensity, causing devastating effects across multiple countries. These storms lead to long-term socio-economic and environmental consequences throughout the region. Cyclones often trigger heavy precipitation and flooding in low-lying areas, disrupting livelihoods, displacing populations, and damaging critical infrastructure (Reason & Keibel, 2004).

The coastal areas of Tanzania, Kenya, and Mozambique are heavily influenced by their proximity to the Indian Ocean. Warm SSTs drive moisture-laden monsoonal winds that increase humidity and contribute to frequent precipitation events. These regions are particularly vulnerable to tropical cyclones, bringing torrential rains and widespread flooding (Chang'a et al., 2020; Kijazi & Reason, 2009). In Mozambique, major river basins such as the Zambezi and Limpopo are especially prone to flooding during these events, exacerbating the country's climate vulnerability.

Moreover, urban areas in countries like Kenya, Tanzania, and Mozambique are particularly vulnerable to flooding due to the rapid pace of urbanization, which has outpaced the development of proper drainage systems. Nairobi, Dar es Salaam, and Maputo have all experienced severe urban flooding in recent years, leading to economic losses and the displacement of vulnerable populations living in informal settlements.

2.2. Data

The analysis of spatial and temporal trends of extreme precipitation in Eastern Africa during January 1981-2023 relies on a comprehensive dataset that includes precipitation, SST, wind components, vertical velocity, and specific humidity. These datasets were selected based on their high resolution, accuracy, and extensive temporal coverage, providing a thorough understanding of precipitation dynamics in the region. Advanced statistical and geospatial techniques were applied to process and analyze the data, revealing trends, variability, and relationships with global climatic factors.

Precipitation data were sourced from the Climate Hazards Group InfraRed Precipitation with Stations (CHIRPS) dataset, which offers daily precipitation records at a 0.05-degree resolution from 1981 to 2023. CHIRPS blends satellite imagery with in-situ measurements, making it particularly valuable in Eastern Africa, where ground-based observations are sparse. The dataset was used to derive extreme precipitation indices (R10mm, R75p, and SDII) for a detailed assessment of extreme rainfall events.

To improve accuracy, CHIRPS employs a statistical blending approach that merges satellite and ground station data through Cold Cloud Duration (CCD) estimates, climatological calibration, and interpolation techniques like inverse distance weighting (IDW) and kriging. These methods correct biases and improve spatial accuracy by giving more weight to ground-based measurements in areas with dense networks while relying more on satellite estimates in regions with fewer stations. Furthermore, CHIRPS implements rigorous quality control procedures, such as bias correction, data validation, and outlier detection, ensuring the reliability of the dataset for climate studies and extreme weather analysis.

Despite its strengths, CHIRPS has limitations, particularly in mountainous regions where satellite-based infrared estimates struggle to capture orographic precipitation, and in areas with sparse ground observations. Additionally, CHIRPS

tends to underestimate short-lived, high-intensity convective storms due to the limitations of infrared satellite imagery. Nonetheless, it remains the primary dataset in this study due to its high-resolution coverage, temporal consistency, and suitability for analyzing precipitation trends in data-scarce regions.

SST data were obtained from NOAA's Extended Reconstructed Sea Surface Temperature Version 5 (ERSSTv5). This dataset, known for its long-term continuity and global coverage, provides monthly SST values dating back to 1854. For this study, SST data from December 1980 to 2022 was analyzed to examine the influence of oceanic conditions on January precipitation patterns in Eastern Africa. The dataset had a spatial resolution of 2˚ by 2˚, allowing for an in-depth investigation of teleconnections between global SST anomalies and precipitation variability.

Wind components (zonal and meridional winds) datasets from the NCEP Reanalysis project, representing monthly mean wind speeds, facilitated the analysis of atmospheric circulation patterns influencing precipitation variability. The data include u-wind (east-west) and v-wind (north-south) components, covering a spatial grid with 2.5˚ intervals. The temporal coverage from 1981 to 2023 enabled an assessment of large-scale wind patterns, moisture transport, and convergence zones impacting extreme rainfall in the region.

Vertical velocity (omega) data from NCEP Reanalysis were analyzed to understand atmospheric convection linked to extreme precipitation. Omega values indicate vertical air movement, with negative values associated with rising motion and convective activity, often leading to precipitation. The dataset includes monthly means at various pressure levels from 1000 hPa to 100 hPa.

Specific humidity data, another key atmospheric variable, were utilized to assess moisture availability in the region. Specific humidity, measured in grams of water vapor per kilogram of air, directly influences cloud formation and precipitation processes. These data, spanning from 1981 to 2023, were extracted from the NCEP Reanalysis project and analyzed across multiple pressure levels to evaluate moisture transport patterns.

All of these datasets provided a robust foundation for analyzing extreme precipitation trends in Eastern Africa. The integration of precipitation data with atmospheric and oceanic variables facilitates the identification of the key mechanisms influencing changes in extreme rainfall events and their spatial variability across the region.

2.3. Methodology

This study employed a systematic approach to analyze the spatial and temporal trends of extreme precipitation in Eastern Africa from January 1981 to 2023. The methodology involved data preprocessing, calculation of precipitation indices, statistical analyses, and visualization techniques. These steps ensured data quality, consistency, and accuracy in identifying trends and patterns in extreme precipitation events across the study region.

Preprocessing of the acquired data involved removing outliers, filling missing values using interpolation, and converting the dataset into a uniform grid format. The precipitation data were clipped using shapefiles to exclude areas outside Eastern Africa.

A monthly precipitation analysis was conducted by aggregating daily precipitation values at each grid point, providing a comprehensive dataset that captured seasonal variations. The monthly climatology for the study period was calculated, along with area-averaged mean precipitation and standard deviation, to assess variability. These calculations helped establish baseline precipitation patterns and visualize seasonal fluctuations across Eastern Africa.

Extreme precipitation indices, including R10mm (days with precipitation ≥ 10 mm), R75p (precipitation amount exceeding the 75th percentile), and SDII (Simple Daily Intensity Index), were computed to evaluate the frequency and intensity of extreme rainfall events. These indices were analyzed spatially and temporally to determine patterns of extreme precipitation and their variability. Spatial maps were generated using Python to illustrate the distribution of these indices.

To detect trends in extreme precipitation, statistical analyses were performed using the Mann-Kendall trend test, which identifies monotonic trends in time series data. Sen's Slope Estimator was used to quantify the rate of change, while linear regression models offered a detailed representation and understanding of precipitation trends. Both temporal and spatial trends were examined to determine variations at different locations and timescales. These statistical methods enabled a robust assessment of how extreme precipitation has evolved over the study period.

Furthermore, a composite analysis was conducted to examine the influence of the South Pacific Convergence Zone (SPCZ) on precipitation variability in Eastern Africa. Years were categorized into SPCZ warm and cold phases based on sea surface temperature anomalies (≥0.5˚C for warm years and ≤−0.5˚C for cold years). Anomalies in precipitation, moisture transport, and vertical velocity were analyzed for each phase to assess their impact on extreme precipitation. Spatial maps of these anomalies were generated to reveal the atmospheric circulation and moisture transport mechanisms associated with SPCZ variability.

3. Results and Discussions

3.1. Annual Cycle of Precipitation over Eastern Africa: Temporal Distribution and Standard Deviation of January Rainfall (1981-2023)

The annual cycle of monthly precipitation over Eastern Africa is illustrated in **Figure 2**, with the bars representing the mean monthly precipitation (in millimeters) and the error bars indicating the standard deviation.

November to April exhibit higher precipitation totals than the other months, with January recording the highest mean precipitation (nearly 200 mm) and the greatest interannual variability, as indicated by its highest standard deviation,

ranging from around 50 mm to 340 mm. The large standard deviation suggests substantial variation in January's rainfall from year to year, indicating significant unpredictability or fluctuations in precipitation patterns.

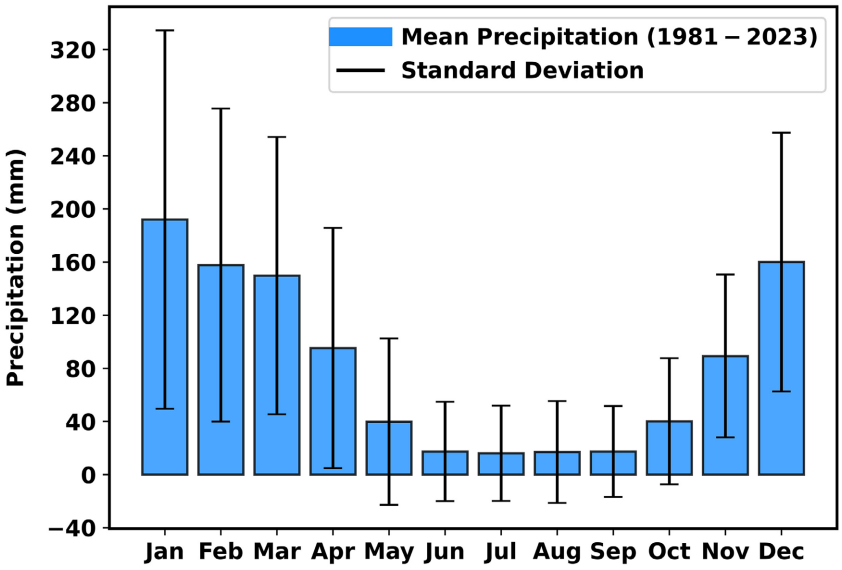

Figure 2. Annual cycle of precipitation over Eastern Africa, illustrating the temporal distribution and standard deviation of monthly rainfall from 1981 to 2023.

Conversely, the period from May through September demonstrates relatively the lowest mean precipitation values, reflecting the region's dry season. This extended dry period, characterized by minimal rainfall, stresses the heightened vulnerability of Eastern Africa to water scarcity, reduced agricultural productivity, and broader socioeconomic challenges during these months. The low standard deviations during this time indicate more consistent precipitation patterns than the wet months. This consistency could facilitate planning for water resource management and dry-season crop scheduling.

In October, precipitation begins to increase, signaling the onset of the rainy season. Rainfall intensifies further from November to January, reaching its peak, and then gradually decreases from February to April, marking the end of the rainy season. December, in particular, exhibits a notable rise in mean precipitation, accompanied by significant variability, as indicated by the error bars. This indicates that while December often experiences substantial rainfall, the amounts can fluctuate significantly from one year to the next.

October to May rains are primarily influenced by the southward migration of the ITCZ, which enhances convective activity. The seasonal precipitation pattern shows that November to April constitutes the primary wet season, with January and February also experiencing notable rainfall, particularly in the southern parts of the region. January's peak rainfall further suggests that not all areas strictly follow the conventional OND and MAM rainfall seasons.

The temporal distribution of precipitation in the Eastern Africa region is char-

acterized by distinct wet and dry seasons. The pronounced variability in precipitation during the wet months, showcases the challenges faced by the region in managing water resources, ensuring agricultural productivity, safeguarding food security, mitigating infrastructure damage, and addressing the impacts of extreme precipitation events.

The annual precipitation cycle over Eastern Africa identified in this study aligns with previous studies. The seasonal transition in rainfall from October to May, driven by the southward migration of the ITCZ, is consistent with findings by Williams and Funk (2011), who linked this migration to shifts in convective activity and large-scale atmospheric circulation patterns. The identification of January as the peak rainfall month, rather than strictly following the conventional OND and MAM rainfall seasons, is supported by Liebmann et al. (2014), who highlighted variability in seasonal onset and intensity across different subregions of Eastern Africa.

3.2. Climatological Spatial Patterns of January Precipitation and Extreme Precipitation Indices (R10mm, R75p, and SDII)

The climatological spatial distributions of January precipitation and the three key extreme precipitation indices (R10mm, R75p, and SDII) were analyzed for January (1981-2023) across Eastern Africa (**Figure 3**). These indices reveal the frequency, intensity, and contribution of extreme rainfall events to total precipitation, aiding in the identification of regional patterns of precipitation variability.

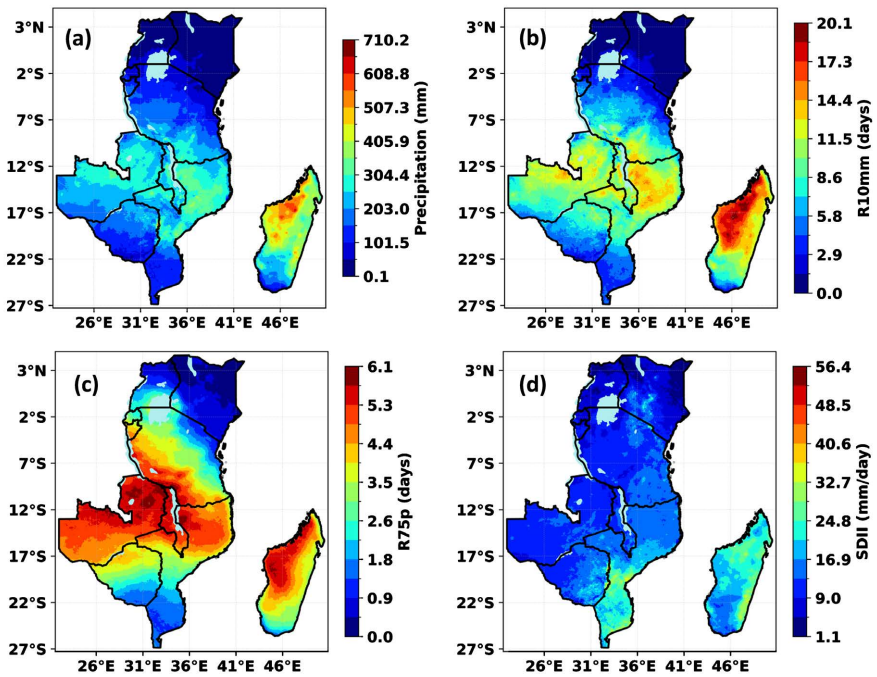

Figure 3. Eastern Africa's January 1981-2023 climatological spatial distributions of (a) January precipitation (mm), (b) R10mm (days), R75p (days), and SDII (mm/day).

The January climatology of precipitation across Eastern Africa for the period 1981-2023 (Figure 3(a)) illustrates that the southern part of the region experiences significantly higher rainfall than the northern part, with precipitation ranging from 0.1 mm to 152 mm in the north and 152 mm to over 700 mm in the south. The rainfall distribution indicates pronounced spatial variations in precipitation patterns, reflecting the diverse climatic conditions across the region.

The R10mm index, which represents the number of days with daily rainfall exceeding 10 mm, identifies areas with frequent moderate to heavy rainfall events. The climatology of R10mm indicates that the highest frequencies ranging from around 7.2 to 20.1 days are observed over the southern parts of the region (Figure 3(b)), particularly Madagascar (except the southern part), Zambia, Malawi, northern Mozambique, northern Zimbabwe, and the southern, southwestern, and western parts of Tanzania. This suggests a higher likelihood of regular moderate to heavy rainfall in these regions during January Moderate frequencies, between 4.3 and 7.2 days, are observed around the Lake Victoria basin, central Zimbabwe and Mozambique, Rwanda, Burundi, southern Madagascar, and Tanzania's central and southern coastal regions, indicating a less frequent occurrence of moderate to heavy rainfall in these areas. In contrast, northern areas, including Uganda, Kenya, the northeastern highlands and extreme northern coast of Tanzania, and the southern parts of Mozambique and Zimbabwe, are relatively drier.

The R75p index, which quantifies the contribution of moderate extreme rainfall events (above the 75th percentile threshold) to total precipitation, further emphasizes the dominance of rainfall in most parts of the southern and southwestern regions (Figure 3(c)), particularly Zambia, Malawi, Burundi, northern Mozambique, northern Zimbabwe, Madagascar (except the southern part), and the southern, southwestern, and western parts of Tanzania. These areas show the highest contributions, indicating their vulnerability to heavy rainfall events during January. Moderate contributions are observed around the Lake Victoria basin, central Zimbabwe and Mozambique, Rwanda, southern Madagascar, and the central and southern coastal regions of Tanzania. This reflects that these areas are relatively less frequently experiencing heavy rainfall events during January. In contrast, northern areas, including northern Uganda, Kenya, the northeastern highlands and northern coast of Tanzania, and the southern parts of Mozambique and Zimbabwe, exhibit much lower contributions, consistent with their lower overall rainfall totals in this month.

The SDII index, which reflects the average intensity of rainfall on wet days, reveals the spatial variability of rainfall strength across Eastern Africa (Figure 3(d)). High rainfall intensities, exceeding 16.9 mm/day, are observed in central and southern Mozambique, parts of Madagascar, and eastern Zimbabwe. Scattered areas of light to moderate rainfall intensities are observed in eastern Tanzania and southwestern Kenya, indicating that wet days in these regions are characterized by relatively frequent but less intense rainfall events. In contrast, the northern parts of the region, including northern, western, and central parts

of Tanzania, Uganda, northern and eastern Kenya, Zambia, Malawi, western Zimbabwe, Rwanda, Burundi, northern Mozambique, and some areas of southern Madagascar, experience lower rainfall intensities, ranging from around 1.1 to 16.9 mm/day. These areas generally experience less intense rainfall events on wet days.

This distribution is in line with the seasonal shifts of the ITCZ and other atmospheric systems that influence rainfall patterns across the region during this period.

3.3. Temporal Trends of Rainfall Characteristics over Eastern Africa (January 1981-2023)

The temporal trends of January precipitation and extreme rainfall indices (R10mm, R75p, and SDII) for January across Eastern Africa from 1981 to 2023 are illustrated in Figure 4. The analysis of January precipitation trends (Figure 4(a)) reveals a statistically significant increase, indicating potential shifts in the region's rainfall patterns during the study period. The findings demonstrate a consistent upward trend, suggesting that January precipitation has intensified over time. This trend is visually evident and supported by robust statistical analyses, confirming the reliability and significance of the results.

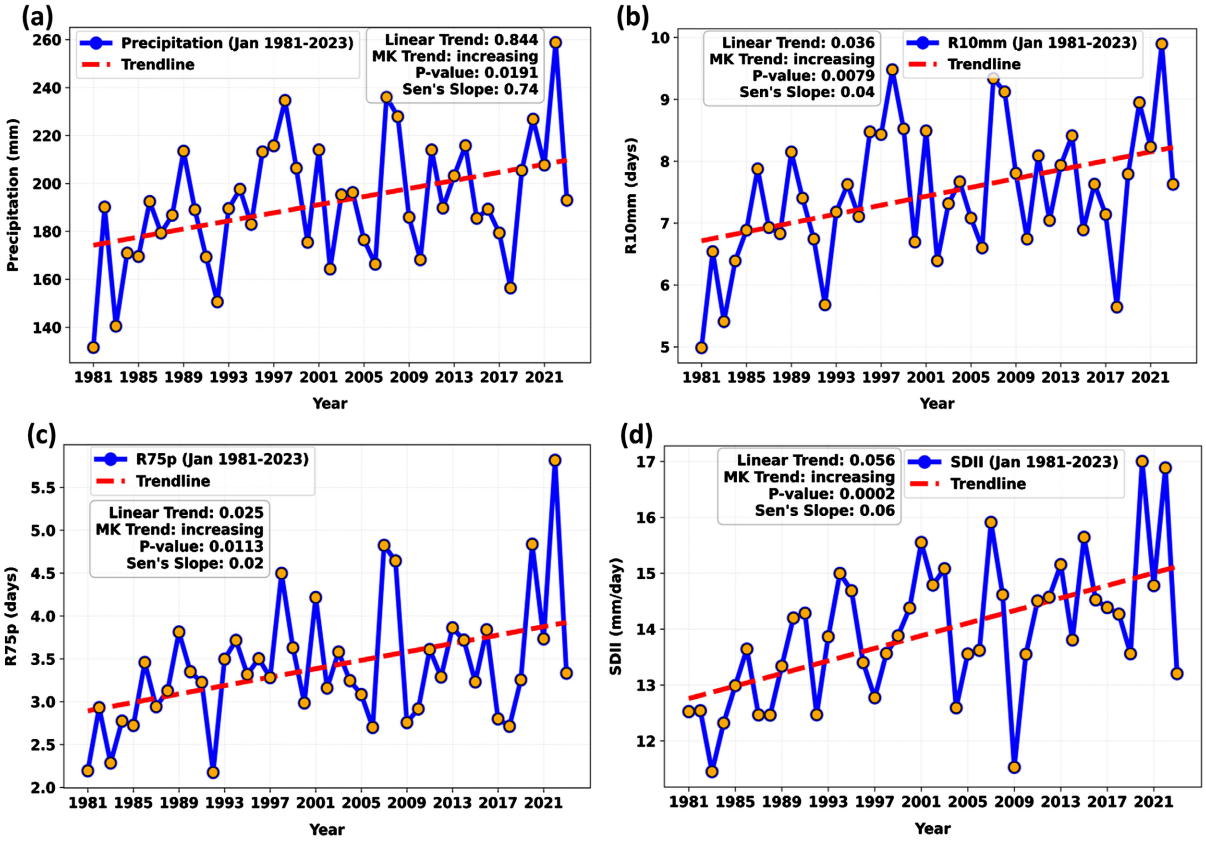

Figure 4. Temporal trends of January (1981-2023) precipitation and extreme rainfall indices across Eastern Africa, based on the Mann-Kendall Test: (a) January precipitation (b) R10mm, (c) R75p, and (d) SDII.

A linear regression analysis of the data shows an overall increase in January precipitation, with a slope of 0.844 mm per year. This steady upward trend is represented by the red dashed trendline, providing a clear depiction of increasing precipitation over 43 years. This suggests a progressive shift in precipitation dynamics, with January becoming wetter over time. The statistical robustness of this trend is further supported by the Mann-Kendall test, a widely used non-parametric method for detecting monotonic trends in time series data. The Mann-Kendall test yields a *p*-value of 0.0191, confirming that the observed trend is statistically significant at the 95% confidence level. This result allows for the rejection of the null hypothesis, which posits no trend, and reinforces the conclusion of a positive trend in January precipitation over the region.

The magnitude of this trend is further quantified using Sen's Slope estimator, a non-parametric method known for its effectiveness in calculating trend magnitudes in environmental and climatic datasets. Sen's Slope estimate indicates an annual increase of 0.74 mm per year in January precipitation, which provides additional confidence in the identified trend. The agreement between the linear regression and Sen's Slope results further strengthens the consistency and robustness of the findings.

This upward trend in January precipitation has significant implications for extreme precipitation events in the region. As overall precipitation increases, the likelihood of more frequent and intense extreme events grows.

Additionally, three extreme precipitation indices (R10mm, R75p, and SDII) were analyzed to investigate the temporal trends of extreme precipitation in Eastern Africa. These indices represent distinct aspects of extreme rainfall events and are necessary for understanding precipitation dynamics across the region.

The analysis of R10mm days (days with precipitation exceeding 10 mm) for January from 1981 to 2023 reveals a statistically significant increasing trend (**Figure 4(b)**). This trend signifies a notable shift in the region's precipitation patterns, with an increase in the frequency of intense precipitation events. The linear regression analysis indicates an annual increase of 0.036 R10mm days per year, represented by the red dashed trendline. This consistent upward trend reflects the growing frequency of heavy rainfall events in January across the region.

The Mann-Kendall test supports the statistical significance of this trend, with a *p*-value of 0.0079, confirming at the 99% confidence level that the observed increase in R10mm days is not due to random variability but a consistent change in precipitation dynamics. Additionally, Sen's Slope analysis estimates an annual increase of 0.04 R10mm days per year, further validating the findings from the linear regression.

In addition to R10mm, R75p days, which represent days with precipitation exceeding the 75th percentile, also show a statistically significant upward trend over the study period (**Figure 4(c)**). The linear regression analysis reveals an annual increase of 0.025 R75p days per year, indicating a steady rise in the frequency of extreme precipitation events across Eastern Africa. This upward trend suggests

that the region is experiencing a growing intensity of extreme rainfall, which could have significant consequences for hydrological processes such as runoff and water availability.

The Mann-Kendall test shows a *p*-value of 0.0113, indicating statistical significance at the 95% confidence level. This result reinforces the observation of a persistent increase in R75p days across the region. Sen's Slope estimator further calculates an annual increase of 0.02 days per year in R75p days, which aligns with the results from the linear regression and Mann-Kendall tests.

An increasing trend in the standardized precipitation intensity index, Simple Daily Intensity Index (SDII), for January from 1981 to 2023 reflects the variability in the average rainfall intensity on wet days. indicates changes in rainfall intensity over the study period (**Figure 4(d)**). The linear regression analysis shows an annual increase of 0.056 mm/day in SDII, as indicated by the red dashed trendline. This upward trend suggests that rainfall events have become increasingly intense over the study period.

The significance of the SDII trend is further validated by the Mann-Kendall test, which yields a *p*-value of 0.0002, well below the 1% threshold, confirming statistical significance at the 99% confidence level. This result emphasizes the consistency of the observed trend and provides strong evidence of increasing rainfall intensity on wet days across the region. Sen's Slope estimator estimates an annual increase in SDII of 0.06 mm/day per year, supporting the conclusions drawn from both the linear regression and the Mann-Kendall test.

The increasing trends in R75p, R10mm, and SDII emphasize a shift toward more frequent and intense precipitation events in Eastern Africa. This change brings potential benefits, such as improved water availability for agriculture, and negative impacts, including flooding and soil erosion, which increase the region's vulnerability to extreme weather events. The intensification of extreme precipitation further calls attention to the urgent need for adaptive strategies to manage these risks, particularly in mitigating flooding and ensuring agricultural resilience.

The spatial patterns of extreme precipitation indices reaffirm the influence of the ITCZ, moisture advection from the Indian Ocean, and orographic effects in shaping rainfall extremes across Eastern Africa. The observed variations in rainfall intensity reflect the combined effects of large-scale atmospheric circulations and local geographic factors, including elevation and proximity to water bodies. The strong contrasts in R10mm, R75p, and SDII stress the heightened vulnerability of southern and central regions to heavy rainfall events, while northern areas experience lower frequencies and intensities of extreme precipitation.

The increasing trends in January precipitation and extreme rainfall indices (R10mm, R75p, and SDII) over Eastern Africa align with previous studies on regional rainfall variability. The rise in heavy rainfall events is consistent with projections by Shongwe et al. (2011), while findings by Ayugi et al. (2022) further indicate intensified precipitation and growing variability. These results strengthen

the evidence of shifting precipitation patterns and increasing extreme rainfall events in the region.

3.4. Spatial Trends of January Precipitation and Extreme Precipitation Indices for January in Eastern Africa (1981-2023)

The spatial trends of January precipitation and associated extreme precipitation indices in Eastern Africa between 1981 and 2023 are displayed in Figure 5. The spatial map of January precipitation trends (Figure 5(a)) reveals distinct regional variations in both the direction and magnitude of trends. The map illustrates areas with increasing and decreasing rainfall, represented by a color gradient ranging from deep blue (negative trends) to red (positive trends). Areas with significant trends, as determined by the Mann-Kendall test, are marked with black dots, indicating regions where the trends are statistically significant. These patterns showcase the heterogeneous nature of January precipitation variability across the region.

In the southern parts of the study area, particularly parts of Mozambique, northern and eastern Madagascar, northern Zimbabwe, southern Zambia, Malawi, as well as the southern and southwestern areas of Tanzania, significant positive precipitation trends are observed. These regions, highlighted in red and orange, show an increase in January rainfall over the study period, with some areas experiencing the most pronounced upward changes.

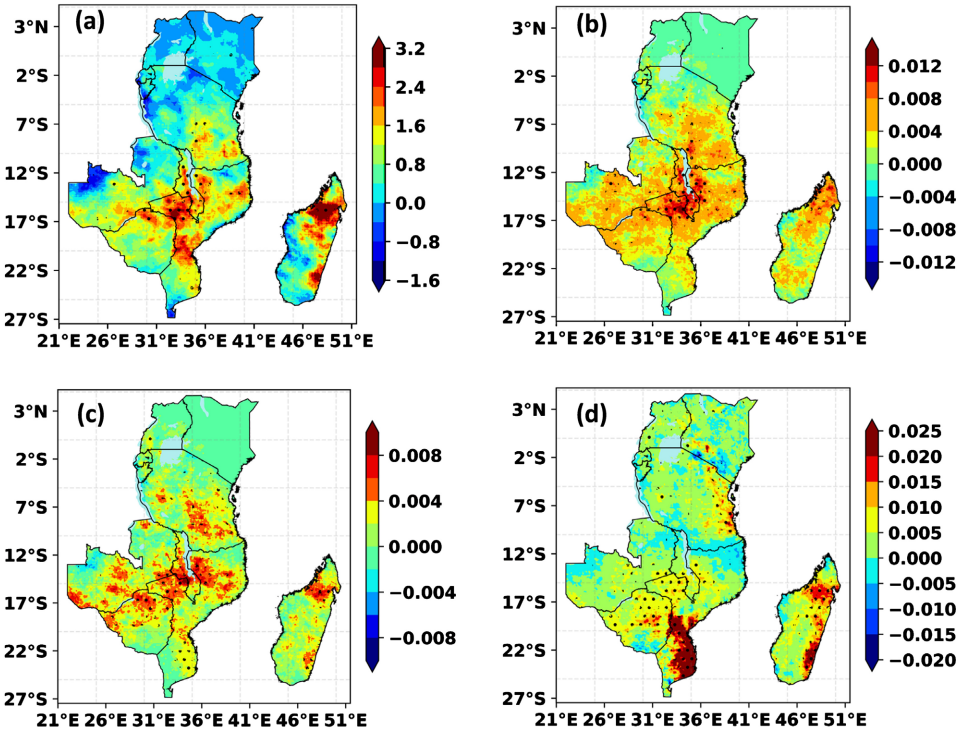

Figure 5. Spatial trends of January (1981-2023) Precipitation and extreme rainfall indices across Eastern Africa based on the Mann-Kendall Test: (a) January Precipitation Trend (mm/year), (b) R10mm Trend (days/year), and (c) R75p Trend (days/year) (d) SDII Trend (mm/day/year).

This trend suggests a general rise in precipitation across these areas, which could have positive and negative implications. While increased rainfall may benefit water resources and agriculture, it could also raise the risk of flooding, soil erosion, and other hazards, particularly in vulnerable regions.

Conversely, the northern and central parts of the study area, particularly Kenya, Uganda, the western and northern to central parts of Tanzania, and parts of Rwanda and Burundi, exhibit predominantly negative precipitation trends. These areas, shown in blue, have experienced a decline in January rainfall over the past four decades, indicating a drying trend. Such changes raise concerns about potential water scarcity and the resulting challenges for agriculture, livelihoods, and sustainable resource management.

The spatial distribution of R10mm trends over Eastern Africa during January from 1981 to 2023 (**Figure 5(b)**) demonstrates significant regional variations in extreme precipitation trends. These differences illustrate areas experiencing increasing and decreasing frequencies of heavy rainfall days.

Regions in the central to southern parts of the study area, including western Mozambique, northern Madagascar, western Zimbabwe, Malawi, parts of Zambia, and some areas in the southern and southwestern Tanzania, exhibit significant positive trends in R10mm, illustrated in shades of yellow, orange, and red. These areas show an increase in the frequency of heavy rainfall days during January. While these upward trends may improve water availability for agriculture, drinking water, and hydropower generation, they also increase the risks of flooding, soil erosion, damage to infrastructure, and displacement of communities, particularly in southern Tanzania, Malawi, northern Madagascar, and western Mozambique.

Conversely, the northern and central parts of the region, including Kenya, Uganda, northern and central Tanzania, Rwanda, and Burundi, show weak to moderate negative and positive trends in R10mm, represented by varying shades of blue and yellow, respectively. Areas with negative trends have experienced a decline in the frequency of heavy rainfall days over the past four decades, indicating drying trends. This decline further raises concerns about water scarcity, diminished agricultural productivity, and increased vulnerabilities for rural livelihoods reliant on consistent rainfall. The observed drying trends in these regions reveal the socioeconomic challenges associated with decreasing water availability, including heightened competition for resources and the potential for conflict.

The spatial distribution of trends in the R75p index (precipitation on very wet days), similarly showcases significant regional differences across Eastern Africa during January from 1981 to 2023 (**Figure 5(c)**).

Regions shaded in yellow, orange, and red indicate an increase in precipitation on very wet days. These include northern and southern parts of Mozambique, southern, coastal, central, western, and southwestern parts of Tanzania, northern and southeastern Madagascar, Malawi, and parts of Zambia and Zimbabwe. While these increases can support agriculture, domestic water supplies, and hydropower

production, they also heighten the risks of flooding, soil degradation, infrastructure vulnerability, and population displacement in areas with pronounced increases.

On the other hand, much of Kenya and Uganda, northeastern Tanzania, and parts of Rwanda, Burundi, and western Zambia exhibit weak to moderate negative trends in R75p, shaded in varying intensities of blue and lime. These declines reflect a reduction in rainfall amounts on very wet days, raising concerns about water shortages, declining agricultural productivity, and greater challenges to sustaining livelihoods in arid and semi-arid regions.

The spatial trend plot for the SDII during January from 1981 to 2023 (**Figure 5(d)**) demonstrates significant spatial variability. Positive trends, represented by varying shades of red, indicate an increase in daily rainfall intensity over time, whereas negative trends, depicted in shades of blue, suggest a decrease in rainfall intensity. The dotted areas on the map denote statistically significant trends, emphasizing the reliability of these observed changes. Yellow and green hues represent moderate positive trends, whereas cyan and light blue indicate slight negative trends.

Areas with deep red shading, such as coastal areas and northeastern parts of Tanzania, northern and eastern Madagascar, few areas in southwestern Kenya, Zimbabwe, and much of southern Mozambique, demonstrate strong positive trends, suggesting intensifying rainfall events. This intensification is linked to an increased frequency and severity of extreme precipitation, contributing to a higher likelihood of heavy rainfall days, which could exacerbate flood risks and impact water management in these areas.

In contrast, isolated areas with blue shading scattered across the region, particularly in northern Mozambique and parts of Tanzania, Zambia, Rwanda, Burundi, and Kenya, indicate declines in rainfall intensity. This suggests a reduction in the frequency and intensity of extreme precipitation events in these regions, potentially leading to drier conditions and affecting water availability, agriculture, and overall ecosystem health.

The contrast between these positive and negative trends in January precipitation, along with the January R10mm, R75p, and SDII indices, particularly in areas identified as significant by the Mann-Kendall test, demonstrates the spatial variability of extreme precipitation changes across the region. These variations indicate shifts in the frequency and intensity of extreme rainfall events, which could have significant implications for flood risk, water resource management, and agricultural sustainability.

Our analysis validated the consistency and robustness of the results by comparing our findings with previous studies on extreme precipitation trends in Eastern Africa. Changes in extreme precipitation under different warming scenarios, as reported by Ayugi et al. (2022), revealed increasing trends in precipitation intensity, a pattern that aligns with our January findings. In a similar vein, an exploration of CMIP5-simulated climate conditions by Otieno and Anyah (2013) high-

lighted growing variability in extreme precipitation across East Africa, which is reflected in our spatial trend analysis. Historical rainfall trends analyzed by Nicholson (2017) and Funk et al. (2019) also indicated an increase in rainfall extremes in certain regions, further supporting our conclusions about heightened flood risks. Additionally, Shongwe et al. (2011) projected intensified heavy rainfall across parts of Africa, mirroring our findings in southern, southwestern, and southeastern parts of Eastern Africa. These studies collectively support the reliability of our results and showcase the growing impact of extreme precipitation in the region.

3.5. Spatial Trends of Specific Humidity (g/kg) and Moisture Transport Vectors and Vertical Velocity for January (1981-2023)

Figure 6 illustrates the spatial trends distribution of specific humidity (q, g/kg) at 850 hPa, along with moisture transport vectors and vertical velocity (Pa/s) for January from 1981 to 2023. The spatial trends of specific humidity overlaid with wind vector trends for January from 1981 to 2023 are displayed in Figure 6(a). The results indicate a clear contrast in moisture trends across the Eastern Africa region. Black dots denote regions where these trends are statistically significant, suggesting an elevated likelihood of extreme precipitation events in these areas.

An increasing trend in specific humidity is observed over southern, western, and southwestern parts of the Eastern Africa region, suggesting an increasing moisture content. In contrast, negative trends are evident over Kenya, northern Uganda, and the northern coast and northeastern parts of Tanzania, pointing to a reduction in atmospheric moisture, which may be linked to long-term drying trends. This spatial divergence suggests that certain areas are experiencing increased moisture availability while others are facing a decline, potentially affecting regional precipitation patterns.

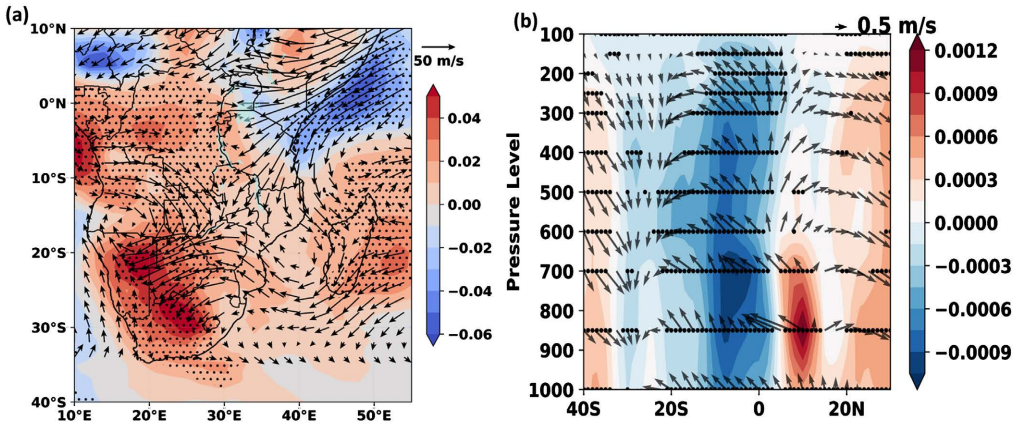

Figure 6. Mann-Kendall trend of (a) specific humidity (shading, g/kg per year) at 850 hPa with moisture transport vector trends (m/s per year), and (b) vertical velocity (omega) trends (shading, Pa/s per year) across pressure levels (hPa), with overlaid zonal-mean meridional and vertical wind trend vectors (m/s per year) for January 1981-2023.

The black wind vectors illustrate changes in moisture transport over time, revealing cyclonic patterns over parts of Zambia, western Tanzania, and the Mozambique Channel extending to western Madagascar. This circulation pattern likely enhances moisture convergence, contributing to increased precipitation in these areas. Additionally, confluent wind patterns are evident over parts of Madagascar, the Lake Victoria Basin, western Zimbabwe, and Zambia, further supporting moisture accumulation and the potential for enhanced rainfall.

The observed drying tendencies may contribute to a decline in extreme precipitation events and an increase in consecutive dry days, affecting agricultural productivity, water availability, and other socioeconomic sectors, such as food security, hydropower generation, and ecosystem stability. Conversely, the increasing moisture trends suggest a higher likelihood of extreme rainfall events, potentially leading to flooding and associated hazards such as soil erosion, infrastructure damage, displacement of populations, and waterborne disease outbreaks. These extreme precipitation events could disrupt transportation networks, overwhelm drainage systems, and negatively impact urban and rural settlements. Furthermore, increased moisture availability may alter regional hydroclimatic patterns, influencing river discharge and groundwater recharge, which could have positive and negative implications for water resource management.

Figure 6(b) presents the vertical trends in atmospheric circulation and pressure-level anomalies for January from 1981 to 2023, illustrating the large-scale atmospheric dynamics influencing extreme precipitation trends in Eastern Africa and adjacent regions. The color shading represents the linear trend in vertical velocity, where negative values (shaded in blue) indicate enhanced upward motion (rising air), which is associated with convection and increased precipitation, while positive values (shaded in red) represent increasing downward motion (subsidence), which is linked to drying conditions and suppressed convection. The overlaid arrows depict the meridional and vertical wind components, showing the changes in the circulation patterns over time. The y-axis represents the atmospheric pressure levels, ranging from 1000 hPa (near the surface) to 100 hPa (in the upper troposphere), while the x-axis represents latitude, covering the equatorial and subtropical regions.

A distinct feature in this figure is the strong upward motion trend over the equatorial region, particularly between 15˚ S and 2˚ N, covering the southern, southeastern, and southwestern parts of the region. In these areas, significant negative vertical velocity trends extend from the lower levels near the surface up to the upper troposphere, indicating an increasing tendency for convection. The significant rising motion trends (marked by black dots) align with observed increases in extreme precipitation, suggesting a growing likelihood of heavy rainfall events. This trend reflects strengthening convective activity, which favors the development of deep cloud systems and intense precipitation.

Conversely, a strong positive vertical velocity trend is observed centered around

5˚ N to 15˚ N, indicating increasing subsidence over this latitude. The enhanced downward motion suggests a drying tendency, which suppresses convection and may lead to more frequent dry spells or drought conditions, particularly in Kenya and Uganda.

The strengthening of upward motion over the southern part of the region indicates an increasing trend in extreme precipitation events, while the enhanced subsidence to the north suggests a shift toward drier conditions. This contrasting pattern of rising and sinking motions reflects large-scale atmospheric circulation adjustments, likely driven by changes in the Hadley or Walker circulation over the region. The wind vector trends further emphasize the structural changes in the vertical circulation. The arrows indicate a strengthening of upper-level divergence in ascending regions, which enhances convection and supports the development of extreme precipitation events, such as intense storms and heavy rainfall. Conversely, an enhanced downward transport of air is observed in subsiding regions, reinforcing stable and dry conditions, which can contribute to prolonged dry spells and an increased risk of drought.

The observed moisture transport and vertical velocity trends are strongly influenced by large-scale circulation patterns associated with the Northeast Monsoon and the seasonal position of the ITCZ during January. The strengthening of upward motion and increased moisture availability over the southern, southwestern, and western parts of Eastern Africa coincide with the influence of monsoonal winds, which transport moisture-laden air from the Indian Ocean and the Congo Basin. This convergence supports convective activity and enhances precipitation in these areas. Conversely, the suppressed convection and drying tendencies over northern and northeastern parts of the region align with the position of the ITCZ, which shifts southward during this period, reducing moisture inflow and favoring subsidence.

3.6. Correlation between Extreme Precipitation Indices (R10mm, R75p, and SDII) and Global SST

The Pearson correlation coefficients were used to examine the relationship between extreme precipitation indices (R10mm, R75p, and SDII) and global SST over Eastern Africa from January 1981 to 2023, with significant correlations highlighted in various oceanic regions (**Figure 7**). Regions with significant correlations, as tested using the Mann-Kendall test, are marked with black dots.

R10mm shows significant positive correlations with SSTs in the southwestern and southeastern Pacific Oceans and the tropical Atlantic Ocean (**Figure 7(a)**). The southwestern Pacific region corresponds to the SPCZ, a key area of deep convection and atmospheric moisture convergence. Warmer SSTs in these regions enhance atmospheric moisture and convection, leading to more frequent heavy rainfall events in Eastern Africa. However, negative correlations are observed in the far southwestern Pacific, where warmer SSTs are linked to fewer heavy precipitation days.

R75p reveals strong positive correlations in the tropical Atlantic, SPCZ, and the Indian Ocean (Figure 7(b)). These areas show that warmer SSTs increase the frequency and intensity of extreme precipitation events. In contrast, some regions in the southwestern and far southeastern Pacific show negative correlations, suggesting that higher SSTs may suppress extreme precipitation due to changes in atmospheric circulation.

SDII demonstrates strong positive correlations with SSTs in the Indian Ocean, some regions in the western and eastern Pacific Oceans, and the Atlantic Ocean (Figure 7(c)), implying that higher SSTs intensify rainfall over Eastern Africa. Negative correlations are observed in the southwestern Pacific, indicating that cooler SSTs are linked to increased precipitation intensity in the region.

Although multiple oceanic regions exhibit significant correlations with extreme precipitation indices, the SPCZ (the region labeled "A" in Figure 7) emerges as the most persistent and influential driver of rainfall variability in Eastern Africa. Other regions, including the tropical Atlantic, eastern Pacific, northwestern Pacific, and Indian Oceans, exhibit notable correlations, but their influence appears more variable and less consistent across different indices. Notably, the SPCZ consistently displays strong correlations, accurately capturing the precipitation patterns in the study region. Given the high correlation between R10mm and other extreme precipitation indices (R75p and SDII), R10mm is used as a representative index to analyze the SPCZ's influence on precipitation variability. To further investigate this relationship, Figure 8 illustrates the distinct anomalies in R10mm precipitation, moisture transport, and vertical velocity associated with SPCZ warm and cold years, pointing out their direct impact on rainfall distribution over Eastern Africa.

3.6.1. Impact of SPCZ Warm and Cold Years on Precipitation Anomalies in Eastern Africa

To assess the influence of SPCZ variability on precipitation patterns over Eastern Africa, precipitation anomalies for January (1981-2023) were analyzed during SPCZ warm (≥0.5˚C) and cold (≤−0.5˚C) years. The SST anomalies defining SPCZ warm and cold years were computed for December (1980-2022). The SPCZ warm years identified are 1988, 1996, 1998, 2005, 2008, 2010, 2011, 2013, 2018, 2020, 2021, and 2022, while the SPCZ cold years include 1980, 1982, 1983, 1984, 1986, 1987, 1989, 1991, 1992, 1994, 1997, 2006, 2014, and 2015.

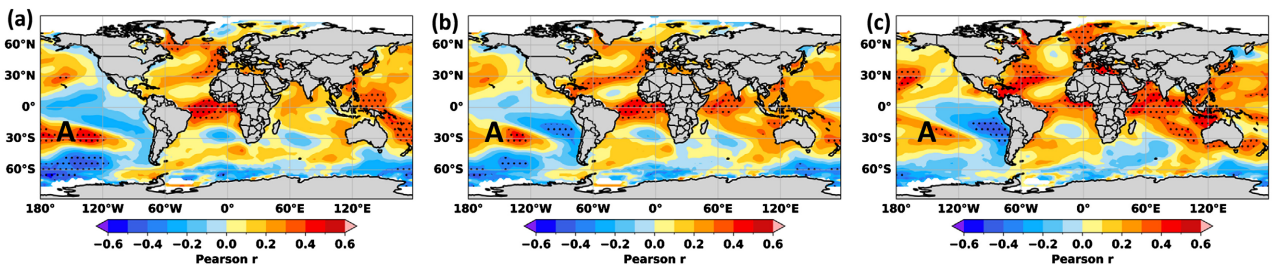

Figure 7. Correlation between extreme precipitation indices (a) R10mm, (b) R75p, and (c) SDII, and Global SSTs.

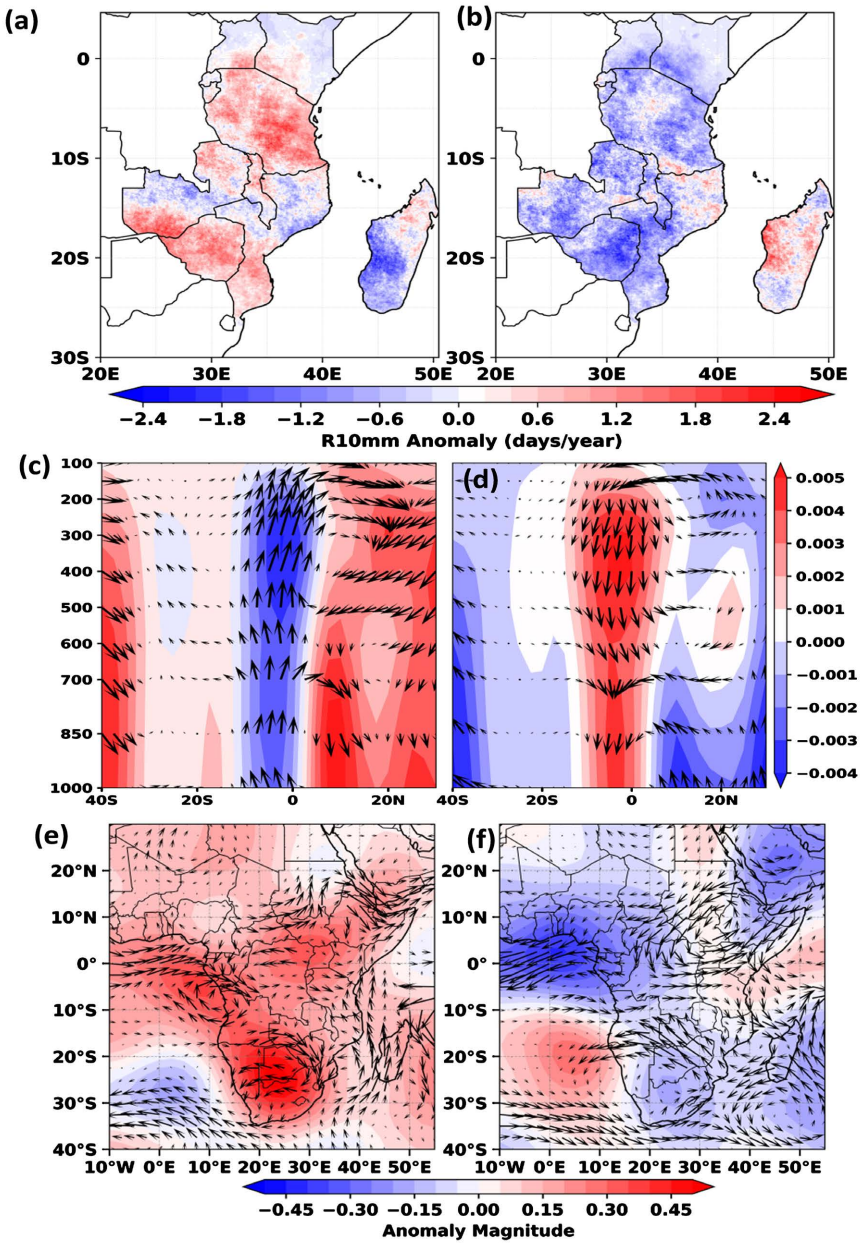

Figure 8. Composite anomalies during SPCZ warm (left) and cold (right) years (defined in December), showing their impact on precipitation and atmospheric circulation in Eastern Africa (January 1981-2023). (a, b) R10mm anomalies (days/year), (c, d) vertical velocity (shading, 10^{-2} Pa/s) with meridional wind vectors (m/s) across pressure levels (hPa), and (e, f) moisture transport ($kg \cdot m^{-1} \cdot s^{-1}$) at 850 hPa, with shading for specific humidity (g/kg) and arrows for wind anomalies.

R10mm anomalies, moisture transport anomalies, and vertical velocity anomalies during SPCZ warm and cold years (January 1981-2023), illustrate the significant influence of SPCZ on extreme precipitation in Eastern Africa (Figure 8).

Figure 8(a) depicts the anomalies in the number of days exceeding 10 mm of precipitation (R10mm) during SPCZ warm years. A shift towards wetter conditions is observed across most of Eastern Africa, with widespread positive anoma-

lies indicating more extreme precipitation days. The most significant increases, exceeding +2.4 days/year, are concentrated in Tanzania, Zimbabwe, southern Mozambique, and parts of Zambia. However, Madagascar experiences negative precipitation anomalies in the southern part, where reductions reach below −1.2 days/year. This indicates that SPCZ warm phases enhance moisture transport and convection over mainland Eastern Africa, leading to wetter conditions, while causing drier conditions over southern Madagascar.

Conversely, Figure 8(b) illustrates the spatial distribution of R10mm anomalies during SPCZ cold years. The results indicate a significant decrease in precipitation across most of the region. The strongest reductions in precipitation are observed in Zimbabwe, southern Mozambique, Uganda, Kenya, and most parts of Tanzania, with anomalies reaching below −2.4 days/year. However, localized positive precipitation anomalies are evident in parts of Madagascar, where precipitation increases up to approximately +1.8 days/year. The results suggest that SPCZ cold phases are associated with drier conditions over mainland Eastern Africa, likely due to suppressed convection and reduced moisture transport.

3.6.2. Vertical Velocity Anomalies during SPCZ Warm and Cold Years

Figures 8(c) and Figure 8(d) demonstrate the vertical velocity anomalies (Pa/s) during SPCZ warm and cold years, respectively, illustrating the atmospheric circulation differences associated with changes in the SPCZ. The shading represents vertical velocity anomalies, where blue indicates negative values (upward motion), which are associated with enhanced convection and precipitation, and red signifies positive values (downward motion), which are linked to suppressed convection and drier conditions.

Figure 8(c) shows a pronounced upward motion in the central region, particularly around the southern latitudes, suggesting intensified convective activity and an increased likelihood of extreme precipitation in these areas. In contrast, during the SPCZ cold years (Figure 8(d)), these areas experienced a dominant downward motion, signifying suppressed convection, enhanced atmospheric stability, and a corresponding reduction in rainfall.

Wind vectors overlaid on both panels illustrate circulation patterns. In the warm SPCZ years, enhanced convergence supports stronger ascent, promoting precipitation, whereas in cold years, increased subsidence limits convective development, leading to drier conditions. This demonstrates how SPCZ variability significantly influences extreme precipitation in the region.

3.6.3. Moisture Transport Anomalies during SPCZ Warm and Cold Years (January 1981-2023)

Figures 8(e) and Figures 8(f) present the composite anomalies of moisture transport during SPCZ warm and cold years, respectively, based on January data from 1981 to 2023. The shading represents specific humidity anomalies (q, in g/kg), while the arrows indicate wind anomaly vectors. The analysis reveals atmospheric moisture flux variations and their potential influence on precipitation patterns over

Eastern Africa.

During SPCZ warm years, characterized by positive SST anomalies (≥0.5˚C), there is a notable increase in moisture transport across most of the Eastern Africa region (Figure 8(e)). The positive specific humidity anomalies (red shading) indicate enhanced moisture availability. The southwestern region and the Lake Victoria basin exhibit relatively higher moisture levels than other areas. The wind anomaly vectors indicate a strong convergence of moisture-laden air and cyclonic flow patterns over the southwestern part of the region. Additionally, the convergence of moist wind patterns is evident over southern, southwestern, and northern coast parts of Tanzania and northern Madagascar, which may contribute to increased convective activity and precipitation in these areas. This pattern suggests a more active hydrological cycle with a higher likelihood of extreme precipitation events.

Conversely, during SPCZ cold years, associated with negative SST anomalies (≤−0.5˚C), the moisture transport patterns exhibit significant reductions in specific humidity (blue shading) over the Eastern Africa region (Figure 8(f)). The wind anomalies indicate a shift in circulation, with an apparent divergence over western Tanzania and the southwestern parts of the region. Furthermore, the ridge system is seen over southern and northern Madagascar and the northern part of the region. This condition suggests reduced moisture influx, suppressing convective activity and potentially leading to a decrease in precipitation, increasing the likelihood of prolonged drier conditions over these areas. However, convergence patterns over northern Madagascar may counteract this trend, promoting enhanced convective activity and potentially leading to increased precipitation in the region.

The observed differences in moisture transport between SPCZ warm and cold years illustrate its role in modulating large-scale ocean-atmosphere interactions and influencing precipitation extremes over Eastern Africa. The increased moisture convergence during SPCZ warm years supports enhanced rainfall, potentially leading to extreme precipitation events. In contrast, SPCZ cold years are characterized by moisture divergence and reduced precipitation, increasing the risk of drought conditions. This emphasizes the strong teleconnections between the SPCZ and Eastern African rainfall variability, contributing to the broader understanding of regional climate dynamics and extreme precipitation trends. It also reinforces the necessity of accounting for SPCZ-related influences in climate trend assessments.

This analysis confirms that SPCZ variability significantly modulates extreme precipitation trends in Eastern Africa. Therefore, changes in SPCZ-related SST patterns can serve as key indicators for predicting extreme precipitation events, improving seasonal forecasts, and enhancing climate resilience strategies in the region.

4. Conclusion and Recommendations

4.1. Conclusion

This study examines the spatial and temporal dynamics of extreme precipitation

in Eastern Africa from January 1981 to 2023, focusing on key precipitation indices such as R10mm, R75p, and SDII. The analysis reveals significant trends in the frequency and intensity of extreme precipitation events, indicating the region's increasing vulnerability to extreme weather. Key findings include:

1) Temporal Trends: Statistically significant increasing trends in January precipitation and extreme precipitation indices (R10mm, R75p, and SDII) signal a rise in the frequency and intensity of extreme precipitation events, which may exacerbate the severity of weather-related challenges across the region.

2) Spatial Variations: Positive trends in extreme precipitation were observed in southern regions, including parts of Mozambique, Madagascar, Malawi, Zambia, Zimbabwe, and southern Tanzania. In these areas, increases in extreme rainfall are likely to exacerbate flooding, waterlogging, and soil erosion, leading to significant disruptions in agriculture, infrastructure, and local economies. The frequent occurrence of such events could increase vulnerability to crop failure, as much of the population in the region relies on rain-fed agriculture, and strain water management systems. Furthermore, these hydrological impacts could lead to displacement of communities, damage to infrastructure, and increased economic losses, further deepening food insecurity and hampering development efforts. In contrast, northern and central regions exhibited mixed trends, suggesting varied impacts on resources and livelihoods throughout the region. These spatial differences reflect the varied climatic influences and localized effects of extreme precipitation events across Eastern Africa.

3) Global SST Influence: The study reveals that global SSTs are significantly linked to extreme precipitation patterns in Eastern Africa. Higher SSTs in the tropical Atlantic, Indian Ocean, and Pacific enhance moisture availability and convection, amplifying the frequency and intensity of extreme precipitation events.

4) Role of SPCZ Variability: A key finding of this study is the dominant influence of the SPCZ on extreme precipitation in Eastern Africa. SPCZ warm years correspond with widespread positive precipitation anomalies across most parts of the region, while SPCZ cold years are generally associated with drier conditions over mainland Eastern Africa. These results indicate that variations in SPCZ-related SST patterns serve as a key driver of rainfall variability. The observed links between SPCZ variability and extreme precipitation trends emphasize its potential as a predictor for seasonal precipitation anomalies in Eastern Africa. Changes in SPCZ-related SSTs are important factors to be considered when forecasting extreme precipitation, improving early warning systems, and informing climate adaptation measures. Given the increasing intensity of extreme rainfall events in the region, integrating SPCZ-based forecasting into climate resilience strategies can enhance preparedness for weather extremes and reduce socio-economic vulnerabilities

4.2. Recommendations

Given the increasing frequency and severity of extreme precipitation events in

Eastern Africa, it is imperative to adopt proactive measures to mitigate impacts and build resilience in the region. The following initiatives are essential to addressing these challenges and improving preparedness across the region:

i) Strengthening monitoring systems through the establishment of robust meteorological networks and satellite-based remote sensing technologies can enhance the prediction of extreme events and improve early warning systems.

ii) Investments in climate-resilient infrastructure, particularly in urban areas prone to flooding, such as Nairobi, Dar es Salaam, Kampala, and Maputo, are essential to reduce risks related to inadequate drainage and rapid urbanization.

iii) Promoting sustainable land management practices, reforestation, and soil conservation will help mitigate flood risks and enhance natural resilience.

iv) Integrating climate adaptation strategies into national development plans, and fostering regional collaboration like the East African Community (EAC) framework, will facilitate resource sharing and address cross-border challenges.

v) Enhancing early warning systems tailored to regional weather patterns, alongside raising awareness and empowering local communities to engage in adaptation planning, will ensure better preparedness for extreme precipitation events.

vi) Encouraging further research on climate variability and extreme precipitation while extending the analysis to other months for a more comprehensive understanding of year-round precipitation patterns. Conducting in-depth research on the links between extreme precipitation events and climate variability will provide a deeper understanding of evolving climate risks in Eastern Africa. Studies should focus on the role of global and regional climate drivers, including SST anomalies, atmospheric circulation patterns, and land-atmosphere interactions, to enhance predictive capabilities and inform climate adaptation strategies. Given the demonstrated influence of SPCZ dynamics on regional rainfall, future research should explore how SPCZ-related SST anomalies drive regional precipitation variability. Understanding the interactions between land-atmosphere processes, large-scale circulation patterns, and SPCZ dynamics will improve seasonal forecasting and early warning systems. Strengthening collaborations between universities, research institutions, and meteorological agencies is so necessary to generate knowledge and develop innovative solutions for climate resilience in the region.

Acknowledgements

The authors acknowledge the conducive research environment and infrastructure at NUIST. The lead author, Masunga Daniel Jonathan, is grateful to the Ministry of Commerce (MOFCOM) of the People's Republic of China for its financial support during the pursuit of a Master's degree at NUIST. Additionally, he acknowledges the valuable guidance and contributions of Prof. Zhang Ling in this research.

Conflicts of Interest

The authors declare that there are no conflicts of interest related to this research.

No financial or personal relationships have influenced the findings in this study.

References

Allan, R. P., Soden, B. J., John, V. O., Ingram, W., & Good, P. (2010). Current Changes in Tropical Precipitation. *Environmental Research Letters, 5,* Article 025205. https://doi.org/10.1088/1748-9326/5/2/025205

Anyah, R. O., & Semazzi, F. H. M. (2004). Simulation of the Sensitivity of Lake Victoria Basin Climate to Lake Surface Temperatures. *Theoretical and Applied Climatology, 79,* 55-69. https://doi.org/10.1007/s00704-004-0057-4

Ayugi, B., Jiang, Z., Iyakaremye, V., Ngoma, H., Babaousmail, H., Onyutha, C. et al. (2022). East African Population Exposure to Precipitation Extremes under 1.5˚C and 2.0˚C Warming Levels Based on CMIP6 Models. *Environmental Research Letters, 17,* 044051. https://doi.org/10.1088/1748-9326/ac5d9d

Cai, X., Zhang, X., Noël, P. H., & Shafiee-Jood, M. (2015). Impacts of Climate Change on Agricultural Water Management: A Review. *WIREs Water, 2,* 439-455. https://doi.org/10.1002/wat2.1089

Camberlin, P. 2018. Climate of Eastern Africa. In *Oxford Research Encyclopedia of Climate Science* . Oxford University Press. https://doi.org/10.1093/acrefore/9780190228620.013.512

Camberlin, P., & Okoola, R. E. (2003). The Onset and Cessation of the "Long Rains" in Eastern Africa and Their Interannual Variability. *Theoretical and Applied Climatology, 75,* 43-54. https://doi.org/10.1007/s00704-002-0721-5

Chang'a, L. B., Kijazi, A. L., Mafuru, K. B., Nying'uro, P. A., Ssemujju, M., Deus, B. et al. (2020). Understanding the Evolution and Socio-Economic Impacts of the Extreme Rainfall Events in March-May 2017 to 2020 in East Africa. *Atmospheric and Climate Sciences, 10,* 553-572. https://doi.org/10.4236/acs.2020.104029

Conway, D., & Schipper, E. L. F. (2011). Adaptation to Climate Change in Africa: Challenges and Opportunities Identified from Ethiopia. *Global Environmental Change, 21,* 227-237. https://doi.org/10.1016/j.gloenvcha.2010.07.013

Cooper, P. J. M., Dimes, J., Rao, K. P. C., Shapiro, B., Shiferaw, B., & Twomlow, S. (2008). Coping Better with Current Climatic Variability in the Rain-Fed Farming Systems of Sub-Saharan Africa: An Essential First Step in Adapting to Future Climate Change? *Agriculture, Ecosystems & Environment, 126,* 24-35. https://doi.org/10.1016/j.agee.2008.01.007

Di Baldassarre, G., Montanari, A., Lins, H., Koutsoyiannis, D., Brandimarte, L., & Blöschl, G. (2010). Flood Fatalities in Africa: From Diagnosis to Mitigation. *Geophysical Research Letters, 37,* L22402. https://doi.org/10.1029/2010gl045467

Donque, G. (1972). The Climatology of Madagascar. In *Monographiae Biologicae* (pp. 87-144). Springer. https://doi.org/10.1007/978-94-015-7159-3_3

Field, C. B., Barros, V. R., David, J. D., Mach, K. J. et al. (2014). *Climate Change 2014: Impacts, Adaptation, and Vulnerability: Part A: Global and Sectoral Aspects*. https://www.cambridge.org/9781107641655

Funk, C., Pedreros, D., Nicholson, S., Hoell, A., Korecha, D., Galu, G. et al. (2019). Examining the Potential Contributions of Extreme "Western V" Sea Surface Temperatures to the 2017 March-June East African Drought. *Bulletin of the American Meteorological Society, 100,* S55-S60. https://doi.org/10.1175/bams-d-18-0108.1

Haile, G. G., Tang, Q., Hosseini-Moghari, S., Liu, X., Gebremicael, T. G., Leng, G. et al. (2020). Projected Impacts of Climate Change on Drought Patterns over East Africa.

Earth's Future, 8, e2020EF001502. https://doi.org/10.1029/2020ef001502

Hastenrath, S. (2001). Variations of East African Climate during the Past Two Centuries. *Climatic Change, 50,* 209-217. https://doi.org/10.1023/a:1010678111442

Ingeri, C., Wen, W., Sebaziga, J. N., Iyakaremye, V., Ekwacu, S., Ayabagabo, P. et al. (2024). Potential Driving Systems Associated with Extreme Rainfall across East Africa during October to December (OND) Season 2019. *Journal of Geoscience and Environment Protection, 12,* 25-49. https://doi.org/10.4236/gep.2024.127003

IPCC (2021). *Summary for Policymakers. Climate Change 2021: The Physical Science Basis*. Intergovernmental Panel on Climate Change (IPCC).

Jury, M. R. (2013). Climate Trends in Southern Africa (with Erratum). *South African Journal of Science, 109,* 1-11. https://doi.org/10.1590/sajs.2013/980

Kebacho, L. L., Ongoma, V., & Chen, H. (2024). Influence of ENSO, Southern Annular Mode, and IOD on the Interdecadal Change of the East Africa 'Short Rains'. *Climate Dynamics, 62,* 4315-4329. https://doi.org/10.1007/s00382-024-07136-y

Kijazi, A. L., & Reason, C. J. C. (2009). Analysis of the 2006 Floods over Northern Tanzania. *International Journal of Climatology, 29,* 955-970. https://doi.org/10.1002/joc.1846

Lawrence, D., & Vandecar, K. (2015). Effects of Tropical Deforestation on Climate and Agriculture. *Nature Climate Change, 5,* 27-36. https://doi.org/10.1038/nclimate2430

Liebmann, B., Hoerling, M. P., Funk, C., Bladé, I., Dole, R. M., Allured, D. et al. (2014). Understanding Recent Eastern Horn of Africa Rainfall Variability and Change. *Journal of Climate, 27,* 8630-8645. https://doi.org/10.1175/jcli-d-13-00714.1

Mafie, G. K. (2022). The Impact of Climate Change on Agricultural Productivity in Tanzania. *International Economic Journal, 36,* 129-145. https://doi.org/10.1080/10168737.2021.2010229

Mokria, M., Gebrekirstos, A., Abiyu, A., Van Noordwijk, M., & Bräuning, A. (2017). Multi-Century Tree-Ring Precipitation Record Reveals Increasing Frequency of Extreme Dry Events in the Upper Blue Nile River Catchment. *Global Change Biology, 23,* 5436-5454. https://doi.org/10.1111/gcb.13809

Morton, J. F. (2007). The Impact of Climate Change on Smallholder and Subsistence Agriculture. *Proceedings of the National Academy of Sciences, 104,* 19680-19685. https://doi.org/10.1073/pnas.0701855104

Msofe, N. K., Sheng, L., Li, Z., & Lyimo, J. (2020). Impact of Land Use/Cover Change on Ecosystem Service Values in the Kilombero Valley Floodplain, Southeastern Tanzania. *Forests, 11,* Article 109. https://doi.org/10.3390/f11010109

Müller, C., Cramer, W., Hare, W. L., & Lotze-Campen, H. (2011). Climate Change Risks for African Agriculture. *Proceedings of the National Academy of Sciences, 108,* 4313-4315. https://doi.org/10.1073/pnas.1015078108

Niang, I., Ruppel, O. C., Abdrabo, M. A. et al. (2014). *Climate Change 2014: Impacts, Adaptation, and Vulnerability. Part B: Regional Aspects. Contribution of Working Group to the Fifth Assessment Report of the Intergovernmental Panel on Climate Change.* Cambridge University Press.

Nicholson, S. E. (2017). Climate and Climatic Variability of Rainfall over Eastern Africa. *Reviews of Geophysics, 55,* 590-635. https://doi.org/10.1002/2016rg000544

O'Reilly, C. M., Alin, S. R., Plisnier, P., Cohen, A. S., & McKee, B. A. (2003). Climate Change Decreases Aquatic Ecosystem Productivity of Lake Tanganyika, Africa. *Nature, 424,* 766-768. https://doi.org/10.1038/nature01833

Osima, S., Indasi, V. S., Zaroug, M., Endris, H. S., Gudoshava, M., Misiani, H. O. et al.

(2018). Projected Climate over the Greater Horn of Africa under 1.5˚C and 2˚C Global Warming. *Environmental Research Letters, 13,* Article 065004. https://doi.org/10.1088/1748-9326/aaba1b

Otieno, V. O., & Anyah, R. O. (2013). CMIP5 Simulated Climate Conditions of the Greater Horn of Africa (GHA). Part 1: Contemporary Climate. *Climate Dynamics, 41,* 2081-2097. https://doi.org/10.1007/s00382-012-1549-z

Pascale, S., Lucarini, V., Feng, X., Porporato, A., & ul Hasson, S. (2016). Projected Changes of Rainfall Seasonality and Dry Spells in a High Greenhouse Gas Emissions Scenario. *Climate Dynamics, 46,* 1331-1350. https://doi.org/10.1007/s00382-015-2648-4

Pereira, L. (2017). Climate Change Impacts on Agriculture across Africa. In *Oxford Research Encyclopedia of Environmental Science*. Oxford University Press. https://doi.org/10.1093/acrefore/9780199389414.013.292

Plumptre, A. J., Davenport, T. R. B., Behangana, M., Kityo, R., Eilu, G., Ssegawa, P. et al. (2007). The Biodiversity of the Albertine Rift. *Biological Conservation, 134,* 178-194. https://doi.org/10.1016/j.biocon.2006.08.021

Reason, C. J. C., & Keibel, A. (2004). Tropical Cyclone Eline and Its Unusual Penetration and Impacts over the Southern African Mainland. *Weather and Forecasting, 19,* 789-805. https://doi.org/10.1175/1520-0434(2004)019<0789:tceaiu>2.0.co;2

Rowhani, P., Lobell, D. B., Linderman, M., & Ramankutty, N. (2011). Climate Variability and Crop Production in Tanzania. *Agricultural and Forest Meteorology, 151,* 449-460. https://doi.org/10.1016/j.agrformet.2010.12.002

Schlenker, W., & Lobell, D. B. (2010). Robust Negative Impacts of Climate Change on African Agriculture. *Environmental Research Letters, 5,* Article 014010. https://doi.org/10.1088/1748-9326/5/1/014010

Schott, F. A., Xie, S., & McCreary, J. P. (2009). Indian Ocean Circulation and Climate Variability. *Reviews of Geophysics, 47,* RG1002. https://doi.org/10.1029/2007rg000245

Sebaziga, J. N., Safari, B., Ngaina, J. N., & Ntwali, D. (2024). Spatial Variability of Seasonal Rainfall Onset, Cessation, Length and Rainy Days in Rwanda. *Theoretical and Applied Climatology, 155,* 7591-7608. https://doi.org/10.1007/s00704-024-05086-3

Shongwe, M. E., van Oldenborgh, G. J., van den Hurk, B., & van Aalst, M. (2011). Projected Changes in Mean and Extreme Precipitation in Africa under Global Warming. Part II: East Africa. *Journal of Climate, 24,* 3718-3733. https://doi.org/10.1175/2010jcli2883.1

Song, Y., Semazzi, F. H. M., Xie, L., & Ogallo, L. J. (2004). A Coupled Regional Climate Model for the Lake Victoria Basin of East Africa. *International Journal of Climatology, 24,* 57-75. https://doi.org/10.1002/joc.983

Taylor, C. M., Belušić, D., Guichard, F., Parker, D. J., Vischel, T., Bock, O. et al. (2017). Frequency of Extreme Sahelian Storms Tripled since 1982 in Satellite Observations. *Nature, 544,* 475-478. https://doi.org/10.1038/nature22069

Teshome, A., & Zhang, J. (2019). Increase of Extreme Drought over Ethiopia under Climate Warming. *Advances in Meteorology, 2019,* 1-18. https://doi.org/10.1155/2019/5235429

Trenberth, K. (2011). Changes in Precipitation with Climate Change. *Climate Research, 47,* 123-138. https://doi.org/10.3354/cr00953

Vande Weghe, J. P. (2004). *Forests of Central Africa: Nature and Man*. Protea Boekhuis.

Verburga, P., & Hecky, R. E. (2009). The Physics of the Warming of Lake Tanganyika by Climate Change. *Limnology and Oceanography, 54,* 2418-2430. https://doi.org/10.4319/lo.2009.54.6_part_2.2418

Washington, R., James, R., Pearce, H., Pokam, W. M., & Moufouma-Okia, W. (2013). Congo Basin Rainfall Climatology: Can We Believe the Climate Models? *Philosophical*

Transactions of the Royal Society B: Biological Sciences, 368, Article 20120296. https://doi.org/10.1098/rstb.2012.0296

Werth, D., & Avissar, R. (2002). The Local and Global Effects of Amazon Deforestation. *Journal of Geophysical Research: Atmospheres, 107,* LBA 55-1-LBA 55-8. https://doi.org/10.1029/2001jd000717

Williams, A. P., & Funk, C. (2011). A Westward Extension of the Warm Pool Leads to a Westward Extension of the Walker Circulation, Drying Eastern Africa. *Climate Dynamics, 37,* 2417-2435. https://doi.org/10.1007/s00382-010-0984-y